Virtual Prototyping of a Compliant Robotic Wrist

Mario Baggetta
Giovanni Berselli
Dept. of Mech., Energy, Management and Trans. Eng. (DIME)
University of Genova
Genova, Italy
mario.baggetta@unige.it
giovanni.berselli@unige.it

Gianluca Palli
Claudio Melchiorri
Dept. of Electrical, Electronic, Information Engineering
University of Bologna
Bologna, Italy
gianluca.palli@unibo.it
claudio.melchiorri@unibo.it

Abstract—This paper deals with the virtual prototyping of a compliant robotic wrist that is aimed for use in a human-robot collaborative environment. The mobility of the wrist is provided by the use of two pairs of Compliant Transmission Elements (CTEs) actuated by servo-motors and tendon transmission. The virtual prototype of the wrist allows easy testing of the behaviour of the tendon transmission and provides an important aid in selecting the right servo-motors for each application.

Index Terms—virtual prototyping, robotic wrist, compliant mechanism, collaborative robots

I. Introduction

Designed to physically interact with humans in a shared workspace, collaborative robots have seen a significant increase in their use in the last few decades [1]. These types of robots can be used to assist doctors during medical treatment, elderly or disabled people with everyday tasks or even workers with industrial tasks [2]. In the development of collaborative robots possible collisions can occur so the need for safety is one of the main objectives. This goal can be achieved, among other possible solutions, by introducing passive compliance [3]. The introduction of a Compliant Transmission Element (CTE) is an effective way to ensure safety in collaborative tasks and limit damage in case of unwanted impacts. In particular, this article aims to present a virtual prototype of a compliant wrist joint for collaborative robots.

A. Wrist design overview

Among all the other joints that could be present on robotic arms, the wrist represents one of the most critical ones, as its importance for the positioning accuracy of the end effector. In the recent literature, many different solutions have been conceived; for instance, in [4] the authors proposed an under actuated wrist based on adaptive synergies while in [5] a novel wrist joint for prosthetic hand is reported. The design of the wrist presented in this paper is carefully described in the author's previous work [6] and summarized in Fig. 1. The wrist is characterized by two functional modules, one for each of its degree of freedom. The first module consists of the upper and intermediate bodies coupled by two CTEs, while the second module consists of the intermediate and lower bodies coupled by two more identical CTEs, namely flexion/extension and ulnar/radial modules. As shown in Fig. 1, each module
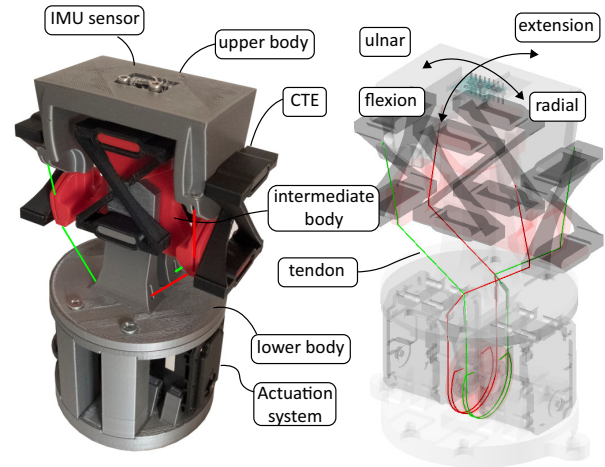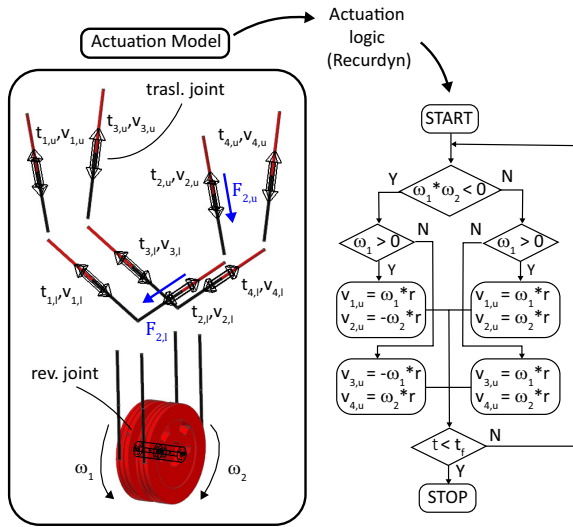

Fig. 1: Compliant wrist prototype.

is actuated by two servo-motors using a set of antagonistic tendons whose routing is highlighted. Using ABS for the CTEs prototipation with the same beam section used in [6] (ABS, with $E = 2.1\,GPa$, $\nu = 0.4$) the maximum deflection of the wrist is equal to ± 60 degrees for the flexion/extension module and ± 30 degrees for the ulnar/radial module.
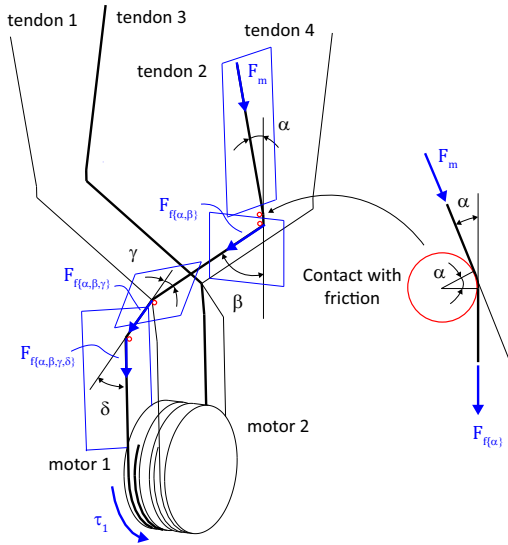
II. Virtual prototyping

In order to simulate the behaviour of the presented wrist during operational tasks, as well as to obtain the appropriate torques to the motors to perform them, a virtual prototype of the wrist has been assembled and tested in a Colink/Recurdyn multisoftware environment.

As shown in Fig. 2a, the actuation system is simulated by using rigid cable sections connected by translational joints that behave like linear actuators. Thus, each tendon is modeled as two different cable sections, the upper one ($t_{1,u}...t_{4,u}$) for the flexion/extension module (whose extremity are fixed to the upper and intermediate bodies) and the lower one ($t_{1,l}...t_{4,l}$) for the ulnar/radial module (whose extremity are fixed to the intermediate and lower bodies). The velocity of each linear actuator is then correlated to the two angular velocities of the motors, ω_1 and ω_2 as shown in Fig. 2a. It

(a) Actuation logic

(b) Friction synthesis

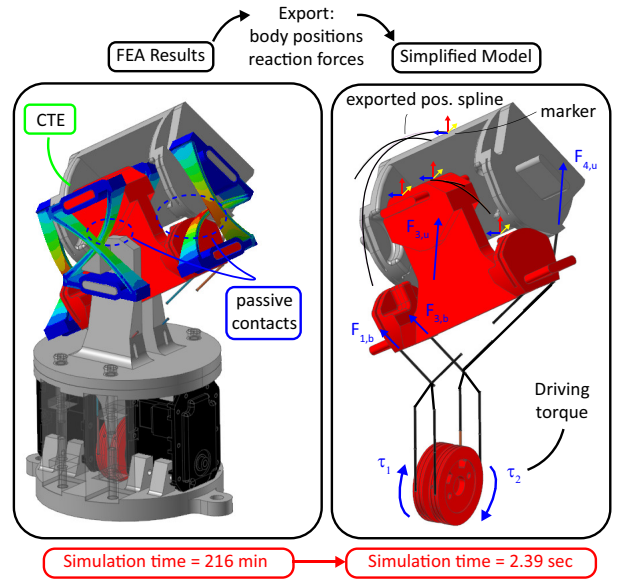Fig. 2: Actuation system implementation

Fig. 3: Simplified model.

bodies. These passive contacts prevent the buckling instability of the CTEs beams when they are subjected to compressed loads. The model thus created requires a computational time of approximately 216 minutes to perform a complete extension/ulnar motion using standard workstation with an Intel(R) Core(TM) CPU @ 2.5 GHz and 16 GB RAM; this much time results unsuitable to be employed in a co-simulation environment. To make a simplified model, as shown in Fig. 3, the position of two markers for each of the two moving bodies (upper and intermediate) was exported as a spline, and then four so-called "point-on-curve" joints were added to the model, binding each marker to move only along its respective exported spline. Following the same principle, all reaction forces measured at the translational joints were exported and added to the model as active forces. This allows both the meshed body and passive contact to be removed from the calculations, resulting in a computational time of 2.49 seconds.

III. SIMULATION CASE STUDY

Finally, a simple control algorithm is tested in a Colink/Recurdyn multisoftware environment. As shown in Fig. 4, this algorithm uses two different PID controllers to tune either the flexion/extension and ulnar/radial modules. The algorithm takes as inputs the set points of the two modules closing the position loop using the wrist feedback positions (given, in its physical counterparts, by an IMU sensor installed on the upper body as shown in Fig. 1). Based on the position error, the algorithm modifies the velocity value of the two servo-motors following the same logic shown in Fig. 2a, making sure to limit it at the maximum value allowed by the tested servo-motors by using a limiter block. It is important to note that the two set points must be reached individually due to the particular cable routing explained in Section 2. For this purpose, the algorithm
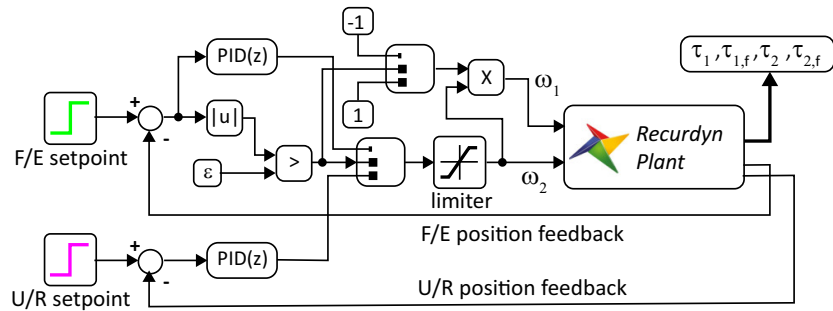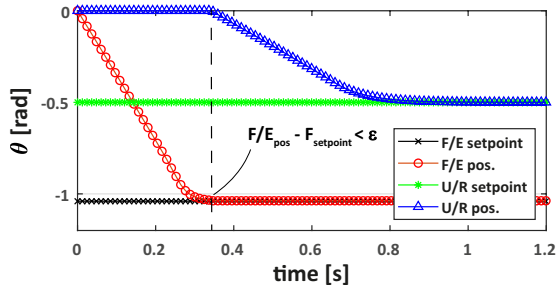
is important to note that the main drawback of this method is the difficulty in modelling the friction effect, which is not the case when it comes to meshed tendon with contact applied. To overcome this problem, all contributions due to friction were mathematically estimated via the Euler-Eytelwein formula [7]:

$$F_{f\{\alpha,\beta,\gamma,\delta\}} = F_m e^{\mu\{\alpha+\beta+\gamma+\delta\}} \tag{1}$$

where $\mu = 0.103$ is the Coulomb friction coefficient [8], F_m is the sum of the reaction forces measured at each couple of translational joints that represent every single tendon (i.e. for tendon 2, $F_m = F_{2,u} + F_{2,l}$ [Fig. 2a]) and $\alpha, \beta, \gamma, \delta$ are the total curvature angles for each of the four contact points that every tendon presents, as shown in Fig. 2b. The virtual prototype of the wrist is then computed by using meshed CTEs and applying passive contacts between the upper and intermediate bodies and between the intermediate and lower

Fig. 4: Colink controller.

Fig. 5: Wrist modules position.

Fig. 6: Driving torques.
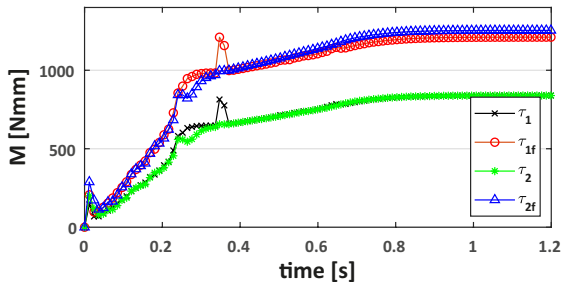

Fig. 7: Wrist application.

activates the ulnar/radial module only if the flexion/extension error is smaller than a user-defined tolerance value ϵ. Figure 5 shows the driving torque of the two servo-motors either neglecting or not the friction contribution. This shows how important it is to take this into account when selecting servo motors, as it involves a significant increase in the required torque. In particular, in the friction-less case, the driving torques on the two motors are equal, whereas, with friction involved, one of the two motors result in being in a slightly disadvantaged position due to the different cable routing.

IV. CONCLUSIONS

A simplified model of a cable-driven compliant robotic wrist is proposed and virtually prototyped using a Colink/Recurdyn multi software environment. This prototype allows to easily test all of the wrist motion possibilities, to safely optimize the
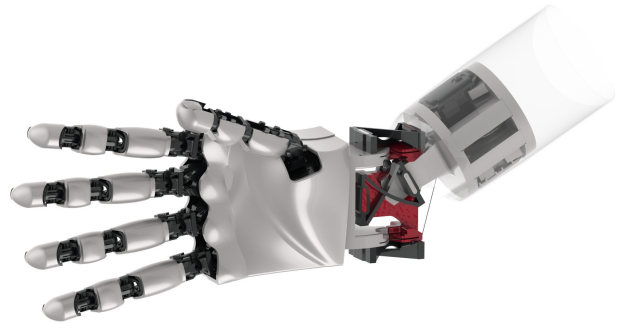
PID controller as well as to determine the torque requirements of the servo motors, even taking friction into account. As a real world application example, Fig. 7 shown the aforementioned wrist assembled on an anthropomorphic robotic arm.

REFERENCES

[1] F. Vicentini, "Terminology in safety of collaborative robotics," *Robotics and Computer-Integrated Manufacturing*, vol. 63, p. 101921, 2020.

[2] A. Cherubini, R. Passama, A. Crosnier, A. Lasnier, and P. Fraisse, "Collaborative manufacturing with physical human–robot interaction," *Robotics and Computer-Integrated Manufacturing*, vol. 40, pp. 1–13, 2016.

[3] F. Guenther, H. Q. Vu, and F. Iida, "Improving legged robot hopping by using coupling-based series elastic actuation," *IEEE/ASME Transactions on Mechatronics*, vol. 24, no. 2, pp. 413–423, 2019.

[4] S. Casini, V. Tincani, G. Averta, M. Poggiani, C. Della Santina, E. Battaglia, M. G. Catalano, M. Bianchi, G. Grioli, and A. Bicchi, "Design of an under-actuated wrist based on adaptive synergies," in *2017 IEEE International Conference on Robotics and Automation (ICRA)*. IEEE, 2017, pp. 6679–6686.

[5] A. A. Elsayed and R. Unal, "Handmech—mechanical hand prosthesis: Conceptual design of a two degrees-of-freedom compliant wrist," in *International Symposium on Wearable Robotics*. Springer, 2020, pp. 107–111.

[6] P. Bilancia, M. Baggetta, G. Berselli, L. Bruzzone, and P. Fanghella, "Design of a bio-inspired contact-aided compliant wrist," *Robotics and Computer-Integrated Manufacturing*, vol. 67, p. 102028, 2021.

[7] G. Palli, G. Borghesan, and C. Melchiorri, "Modeling, identification, and control of tendon-based actuation systems," *IEEE Transactions on Robotics*, vol. 28, no. 2, pp. 277–290, 2011.

[8] P. Bilancia, M. Baggetta, G. Hao, and G. Berselli, "A variable section beams based bi-bcm formulation for the kinetostatic analysis of cross-axis flexural pivots," *International Journal of Mechanical Sciences*, p. 106587, 2021.